Oil & Gas Science and Technology – Rev. IFP, Vol. 61 (2006), No. 4, pp. 547-559

IFP International Conference
Rencontres scientifiques de l'IFP

Research Advances in Rational Design of Catalysts and Sorbents
Avancées de la recherche dans la conception rationnelle de catalyseurs et d'adsorbants

^{35}S Tracer Study of the Effect of Support on the Nature of the Active Sites of Co(Ni)Mo Sulphide Catalysts Supported on Al_2O_3 and Activated Carbon

V.M. Kogan[1] and N.N. Rozhdestvenskaya[1]

1 Zelinskiy Institute of Organic Chemistry, Russian Academy of Sciences,
47, Leninsky prospect, Moscow 119991 - Russia
e-mail: vmk@ioc.ac.ru

Résumé — Étude par traçage isotopique ^{35}S de l'influence du support sur le caractère des sites actifs de catalyseurs sulfurés Co(Ni)Mo supportés sur Al_2O_3 et sur carbone activé — L'influence du support (Al_2O_3 et carbone activé) sur l'activité de catalyseurs Mo, NiMo et CoMo dans l'hydrogènolyse du thiophène est examinée en se servant de ^{35}S comme traceur isotopique. Les sites sont plus actifs dans des catalyseurs supportés sur carbone que dans ceux supportés sur alumine, alors que les fréquences de la rotation de ces sites sont similaires. La désulfurisation du thiophène et l'hydrogénation des oléfines en C_4 résultants se réalisent sur le même site localisé sur le molybdène. Les tests de traçage isotopique ont montré que les sites actifs dans les catalyseurs examinés sont identiques, et que le support n'influe que sur leur concentration.

Abstract — ^{35}S Tracer Study of the Effect of Support on the Nature of the Active Sites of Co(Ni)Mo Sulphide Catalysts Supported on Al_2O_3 and Activated Carbon — *The influence of the support (Al_2O_3 and activated carbon) on the activity of Mo, NiMo, and CoMo catalysts in thiophene hydrogenolysis is studied using ^{35}S as a tracer. The carbon-supported catalysts have more active sites than their alumina-supported counterparts, while the turnover frequencies of these sites are similar. Thiophene desulfurization and the hydrogenation of the resulting C_4 olefins take place at the same Mo sites. Tracer tests have demonstrated that the active sites in the catalysts examined are identical and the support has an effect only on their concentration.*

List of Symbols

A_i	preexponential multiplier
M_S	sulfur atomic mass = 32
M_{Th}	thiophene molecular mass = 84

$N_{Th} = \upsilon\ \rho/M_{Th}$ the number of thiophene mmol in the pulse

$N_S = S_i/M_S$ the number of mmol of mobile sulfur of the given type

P_i	productivity of active site of given type during 1 thiophene pulse
S_i	mobile sulfur amount on the sites of the given type i (mg)
x	H_2S amount formed in the course of thiophene HDS reaction (cm^3)
α	H_2S molar radioactivity normalized to the value of initial one (%)
γ	thiophene conversion (%)
υ	thiophene pulse volume = 1μL
ρ	thiophene density = 1.064
λ_i	exponential power.

INTRODUCTION

Hydrotreating catalysts prepared by loading activated carbon with an active phase (C-supported catalysts) are more active than conventional systems based on Al_2O_3 or SiO_2 [1-9]. After the service life of a C-supported catalyst is over, the metals of the active phase can be recovered by burning out the support and then reused. Furthermore, cobalt in C-supported CoMo catalysts, unlike cobalt in Al_2O_3-supported catalysts, does not react with the support to form a spinel and remains entirely in the active phase. However, there are reasons why C-supported catalysts have found only little industrial application. Firstly, although the C-supported CoMo catalysts show a very high specific activity, their support has a low density and, accordingly, they are inferior to Al_2O_3-supported catalysts in activity per liter (which is an industrially accepted characteristic of a catalyst). Secondly, about 50% of the pore volume in activated carbon is due to micropores, which can limit the diffusion of the reactants.

These are the reasons why C-supported catalysts are primarily interesting as model systems for investigating the effect of the support on the performance of the active phase. Most of the studies in this field have dealt with the structure of catalysts, the effects of the preparation method and support on this structure, and the correlation between these characteristics and catalytic activity [7-13].

X-ray photoelectron spectroscopy (XPS) [14] revealed different types of interaction between the support (Al_2O_3 or activated carbon) and molybdenum sulfide as an active phase. XPS data indicate the presence of MoS_2 and cobalt sulfide species (Co_9S_8, Co-Mo-S, and $CoMo_2S_2$) in sulfided CoMo/C and CoMo/Al_2O_3 catalysts. However, these species are difficult to identify, because they give very similar Co_{2p} spectra [15]. Mössbauer emission spectroscopy and X-ray absorption spectroscopy and EXAFS confirmed the presence of a Co-Mo-S phase in the CoMo/C catalysts [16-19]. The fact that the active phase in the C- supported catalysts is not bound to the support through oxygen atoms suggests that the Co-Mo-S species on carbon differ in properties from the same species on alumina. Two types of Co-Mo-S structure were discovered in Al_2O_3-supported catalysts [20, 21]. Type I structures form at conventional sulfiding temperatures; type II structures form at ordinary or elevated temperatures, but they need special impregnation conditions. The Co-Mo-S structures on activated carbon are type II. This fact is consistent with the assumption that type I Co-Mo-S structures are more strongly bound to the support and, therefore, less active than type II ones [22].

Owing to the strong interaction between the active phase and Al_2O_3, small molybdenum disulfide crystallites are uniformly distributed over the support surface and are stable (primarily in respect of agglomeration) during the catalytic reaction. At the same time, the strong interaction in the Al_2O_3-supported catalysts is disadvantageous: it favors the formation of the low-active (type I) Co-Mo-S structure.

In order to understand the principles of functioning of the active phase on different supports, it is necessary to study the transformations of sulfurorganic compounds on the surface of this phase. A number of recent studies have been devoted to the kinetics of conversion of thiophene and dibenzothiophenes on C-supported Co- and Ni-containing molybdenum sulfide catalysts of various compositions [23-28]. Those studies have dealt with the effects of the partial pressure of hydrogen sulfide, N-containing additives in the reaction mixture, and reaction conditions. It is assumed that desulfurization and hydrogenation sites are different and no quantitative estimates have been reported for the properties of these sites. Application of the radioisotopic technique [29-31] enabled us to determine the number of surface SH groups, evaluate the reactivity of active sites, and correlate these data with the composition of the active phase of the sulfide catalyst. Here, we report a radioisotopic investigation of the dependence of catalyst activity in thiophene hydrogenolysis on the nature of the support.

1 EXPERIMENTAL

1.1 Catalyst Preparation and Pretreatment

We examined four series of Mo catalysts and CoMo and NiMo bimetallic catalysts supported on γ-Al_2O_3 and activated carbon. The molybdenum content of the Mo/Al_2O_3 and Mo/C catalysts was varied between 3 and 12 wt%.

Furthermore, we tested a series of samples containing 10% Mo, varying the Co concentration between 0.5 and 4%. The catalysts were prepared by impregnating γ-Al_2O_3 (specific surface area, 240 m^2/g; pore volume, 0.54 cm^3/g) and coconut carbon (specific surface area, 820 m^2/g; pore volume, 0.46 cm^3/g) with aqueous solutions containing appropriate amounts of ammonium heptamolybdate and nickel (cobalt) nitrate. The impregnated materials were dried at 110°C for 2 h and calcined at 500°C for 3 h.

Prior to tracer tests, the catalysts were sulfided with elementary ^{35}S in a 21 cm^3 autoclave at P = 6 MPa, T = 360°C, and a catalyst-to-sulfur ratio of 5:1 for 1 h.

1.2 Radioisotopic Tests of the Catalysts

A catalyst sample containing radioactive sulfur (25-300 mg) was transferred into a pulsed catalytic microreactor coupled with a radiometric chromatograph *(Fig. 1)*. The catalyst was treated with helium, and the hydrogen flow (chromatographic carrier gas) was switched over to pass through the reactor. This was followed by pulsed injection of 1 μl portions of unlabeled thiophene into the reactor.

The reaction yielded C_4 hydrocarbons and hydrogen sulfide. Radioactivity was detected only in hydrogen sulfide. The molar radioactivity of the resulting hydrogen sulfide gradually decreased with increasing number of thiophene portions injected, because the radioactive sulfur of the catalyst was progressively replaced by the nonradioactive sulfur of thiophene.

Chromatographic analysis of the thiophene conversion products was carried out in two modes. In the first mode, the products were separated into hydrogen sulfide, hydrocarbons, and thiophene to measure the radioactivity of the hydrogen sulfide. In this mode, we used column 1 *(Fig. 1)*, which was packed with 15% Carbowax/Celite 545 (3 mm × 3 m; 120°C).

Analysis of the hydrocarbon fraction was carried out in the second mode. In this mode, after the products were separated in column 1, the hydrocarbon fraction and hydrogen sulfide were collected in trap 2 and then directed to column 2 (12% tributyl phosphate/Chromosorb P; 3 mm × 7.5 m; 25°C). In all the runs the molar percentage of H_2S was equal to the molar percentage of the sum of C_4-hydrocarbons.

The signals from the thermal-conductivity detector and the radiation counter were processed in the on-line mode using the Mul'tikhrom 2.74 program. The radioactivity of hydrogen sulfide was measured with a flow- type proportional radiation counter. The quencher was methane, which was fed into the counter as a 1:1 mixture with the carrier gas.

The sulfur content of ^{35}S-labeled catalyst samples was determined by measuring their specific radioactivity (SR) and comparing it with the SR of the sulfiding agent.

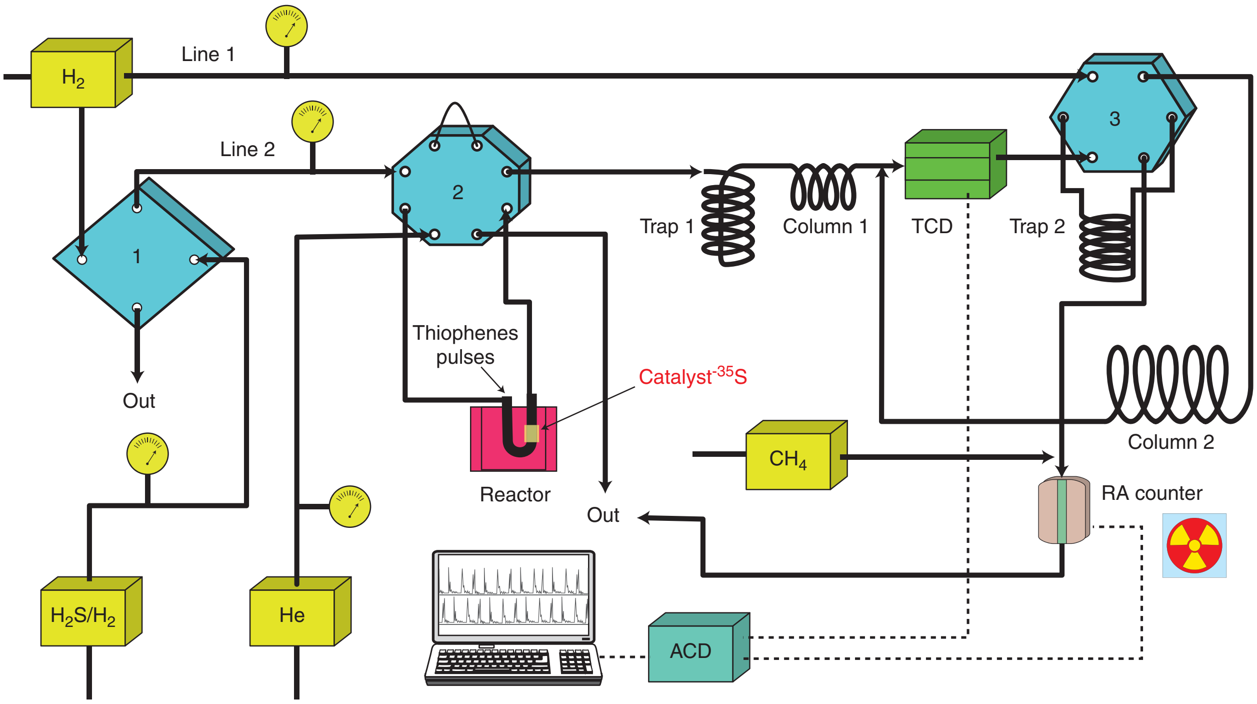

Figure 1

Schematic of the pulsed catalytic setup, including on-line radiochromatographic analysis of the products: (1) four-way valve, (2) eight-way valve, and (3) six-way valve; ADC is an analog-to-digital converter; TCD – thermal-conductivity detector.

1.3 Mathematical Processing of Experimental Data

Curves of H_2S molar radioactivity (MR) as a function of the H_2S produced (cm^3) were calculated, equivalent to the dependence on the amount of reacted thiophene. H_2S MR values were normalized relatively to the value of the initial MR of sulfide sulfur on the catalyst (%). The dependencies obtained can be approximated by exponential equations of the following type:

$$\alpha = \Sigma\, A_i \exp(-\lambda_i x) \tag{1}$$

To approximate experimental curves by a self-consistency method, the Curve Expert 1.34 program was applied. Standard errors less than 1-2% and correlation coefficients better than 0.998 were usually reached after 35-40 iterations.

The exponential form of Equation (1) is determined by the fact that the processes of isotope exchange and replacement are described by first order equations. Each item of (1) describes the H_2S MR changes with an intensity determined by the value of the exponential power λ_i, this intensity being characteristic of active sites of the given type. If it is possible to describe the experimental curve by single-exponential equation, it means that there is only one type of active sites on the catalyst. If a biexponential equation is required, there are two types. Both are responsible for H_2S formation but differ in their SH group mobility. In (1) the pre-exponential multiplier A_i determines the proportion of thiophene converted on the site of the given type. If there is only one type of the sites ($i = 1$) on the catalyst $A_i = 100\%$.

Proceeding from Equation (1), it is possible to estimate the amount of catalyst sulfur (in mg) that can participate in H_2S formation (mobile part of sulfur) on the sites of the given type:

$$S_i = \frac{32}{22.4 \times 100} \int_0^\infty A_i \exp(\lambda_i x)dx \tag{2}$$

Integration of (2) gives:

$$\frac{32}{22.4 \times 100} \times \frac{A_i}{\lambda_i} \tag{3}$$

If more than one exponent describes the curve, *i.e.* if several types of active sites take part in the reaction, the total amount of mobile sulfur is estimated by the sum: $S_{mob} = \Sigma\, S_i$.

If the conversion γ is known, it is possible to estimate the thiophene amount converted on each type of the sites, *i.e.* site productivity P_i. P_i can be calculated as the ratio of the number of converted thiophene molecules to the number of the SH groups of the sites of a given type:

$$Pi = \frac{\gamma}{100} \times \frac{Ai}{100} \times \frac{NTh}{NS} \tag{4}$$

Then:

$$Pi = \frac{\gamma}{100} \times \frac{A_i}{100} \times \frac{\nu\rho}{84} \Big/ \frac{S_i}{32} \tag{5}$$

If we put (3) into (5) and make some simple transformations we obtain:

$$Pi = 2.84 \times 10^{-3} \gamma\ \lambda i \tag{6}$$

We assumed that the maximum amount of mobile sulfur (S_{mob}) on the catalyst is about 40% of the stoichiometric amount of sulfur. This assumption is based on the results of our previous studies [29]. The number of partly reduced sites (PRS) corresponds to the difference between the maximum possible amount of catalyst SH groups and actually measured ones. The number of SH groups determined in the experiment is equal to S_{mob}. So,

$$\Sigma\ \mathrm{PRS} = 0.4\ S_{stoi} - S_{mob} \tag{7}$$

The PRS, that directly participate in the reaction, *i.e.* on which thiophene molecules are adsorbed and react, are named "functioning vacancies", or, simply, vacancies (*V*) and those that do not – "empty sites" (ES).

The number of vacancies V_i can be easily determined from the value of the productivity P_i of the active sites of the type *i*. Indeed, if the active site productivity P_i is the number of the H_2S molecules formed with the participation of an SH group of the given type that means that its reciprocal ($1/P_i$) indicates the number of SH groups of the *i*-type one of which participates in one H_2S molecule formation. As one H_2S molecule formed corresponds to one vacancy V_i, the $1/P_i$ is the ratio of the number of SH groups to the number of vacancies of the given type.

$$1/P_i = \mathrm{SH}_i : V_i \tag{8}$$

If we know P_i and the number of the SH groups of the *i* type (mobile sulfur S_i from Equation (2) or Equation (3)) we can determine the number of the V_i. The sum of "empty sites" is the rest between the total number of the partly reduced sites (Σ PRS) and the number of the functioning vacancies V_i:

$$\Sigma \mathrm{ES} = \Sigma \mathrm{PRS} - \Sigma V_i \tag{9}$$

2 RESULTS AND DISCUSSIONS

After their treating in H_2 flow at the reaction temperature, the catalysts contained less sulfur than before treating because some sulfide sulfur left the catalyst in the form of H_2S during the first minutes of H_2 flow over the catalyst. As a result, the catalyst changed to a partially reduced state and on the surface of the active phase vacancies were formed that could adsorb sulfurorganic compounds in the course of HDS. Further hydrogen treating did not lead to essential quantitative change of the catalyst sulfur content. This phenomenon can be easily understand by attracting the results obtained by Cristol *et al*. [32] according to which sulfur atom desorption from the sulfur edge of MoS_2 under hydrogen flow needs energy twice higher than is necessary for such desorption preceded by the adsorption of sulfurorganic molecule. This means that the share of the cover of the MoS_2 edge by sulfur and the structure of the vacancies depend not so much on hydrogen pressure as on preadsorption of the reactant molecule. Moreover, as it has been shown by Schweiger *et al.* [33, 34], the most stable morphology of the MoS_2 slab edge for unpromoted and promoted by Ni or CoMo catalysts under reaction conditions is the structure where sulfur covers about 50 percent of the edge surface for unpromoted MoS_2 slab or a little bit higher for promoted Co(Ni)Mo slab. This conclusion agrees well with our results [29].

2.1 Unpromoted Catalysts Mo/Al_2O_3 and Mo/C

Experimental data for the Mo/Al_2O_3 and Mo/C catalysts are presented in Figures 2-7. It is clear from Figure 2 that the concentration of mobile sulfur, S_{mob}, and its fraction in the total amount of sulfide sulfur are much greater in the C-supported catalysts than in the Al_2O_3-supported ones. Therefore, both the S_{mob} content and the ratio of surface (mobile) sulfur to bulk (immobile) sulfur depend on the nature of the support.

In the C-supported catalysts, like in Mo/Al_2O_3, the proportion of mobile sulfur decreases as the Mo content is raised. A plausible explanation of this fact is that the molybdenum sulfide phase coarsens with increasing Mo content of the catalyst. However, the shape of the mobile sulfur curve is support dependent. For Mo/Al_2O_3, S_{mob}/S_{tot} decreases monotonically. For Mo/C, this ratio falls markedly between 3 and 6% Mo, while further raising the Mo content does not cause considerable changes in S_{mob} and, accordingly, molybdenum sulfide particle size.

Furthermore, raising the Mo content reduces the SH/PRS ratio *(Fig. 3)*, and the proportion of SH groups decreases much more rapidly in MoS_2/Al_2O_3 than in Mo/C. Comparing the curves plotted in Figures 2b and 3 suggests that SH/PRS and S_{mob}/S_{tot} vary in the same way and the amount of PRS's in the unpromoted Al_2O_3- and C-supported molybdenum catalysts is proportional to the S_{tot} content *(Fig. 4)*.

In our earlier studies [29, 30], we arrived at the conclusion that the PRS's are a totality of functioning vacancies (*V*'s) and empty sites (ES's): $\Sigma \text{PRS} = \Sigma V + \Sigma \text{ES}$. Comparison between Figures 5a and 5b demonstrates that the relative amounts of *V*'s and ES's increase in proportion to the Mo content.

Analysis of these data together with the evaluated catalytic activity data for thiophene hydrodesulfurization *(Fig. 6)* shows that the specific activity of the molybdenum catalyst depends only slightly on the support and the amount of the active phase. Therefore, by changing the support or varying the amount of the active phase, one can only change the number of active sites, not their activity.

Figure 7 shows how the butane:butenes ratio, which is a characteristic of hydrogenating capacity, depends on the density of functioning vacancies (number of *V*'s per 1000 SH groups) for the Mo/Al_2O_3 and Mo/C catalysts. The hydrogenating capacity of these catalysts, like that of catalysts poisoned with N-containing compounds [31], depends linearly on the density of the vacancies responsible for desulfurization. This finding confirms the deduction that thiophene hydrogenation and desulfurization take place at the same sites.

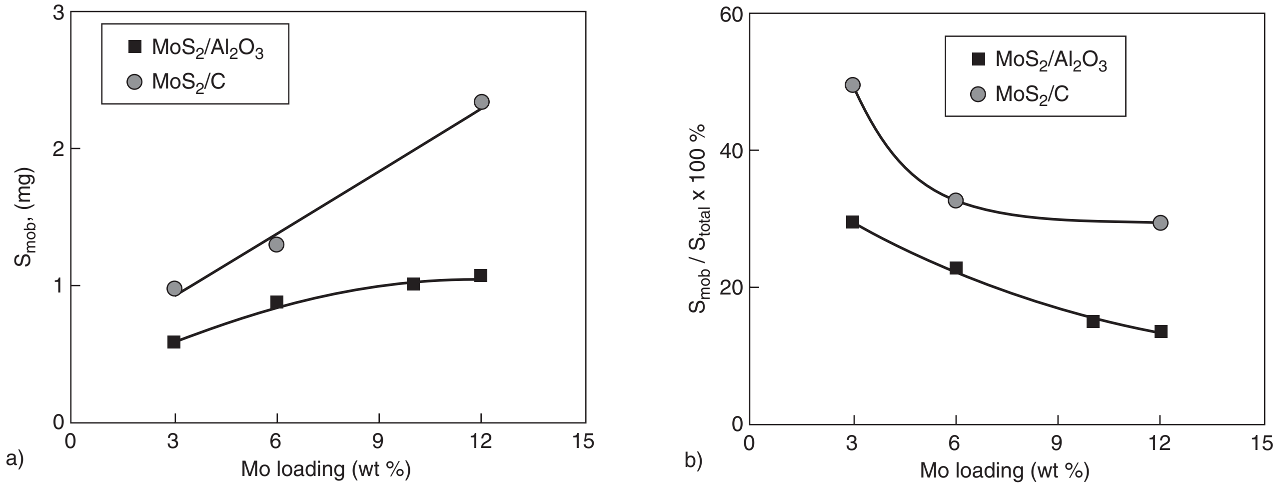

Figure 2

(a) Amount and (b) fraction of mobile sulfur as a function of Mo content for (■) alumina- and (●) carbon-supported molybdenum sulfide catalysts.

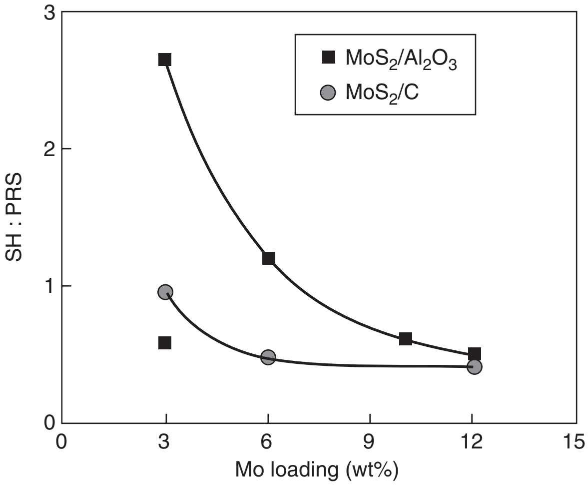

Figure 3

SH/PRS as a function of Mo content for the (■) Mo/Al_2O_3 and (●) Mo/C catalysts.

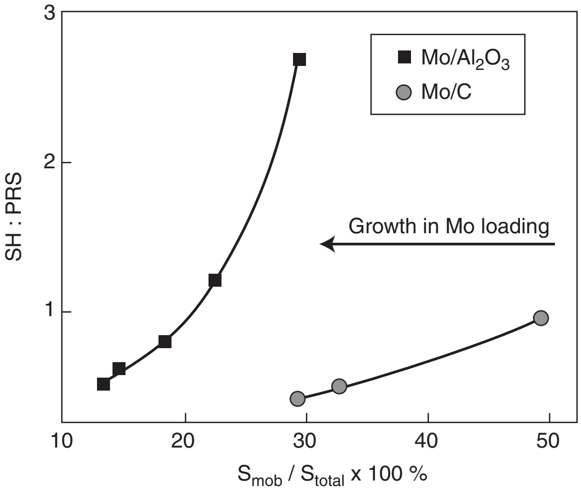

Figure 4

SH/PRS as a function of S_{mob}/S_{tot} for the (■) Mo/Al_2O_3 and (●) Mo/C catalysts with different Mo contents.

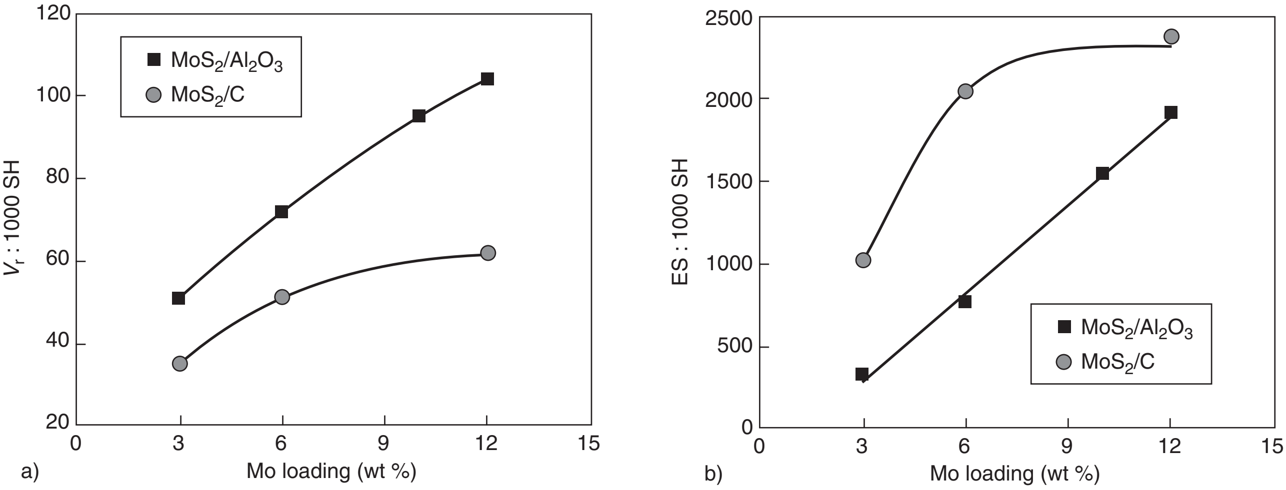

Figure 5

(a) V and (b) ES densities as a function of Mo content for the (■) Mo/Al_2O_3 and (●) Mo/C catalysts.

As compared to the MoS_2/Al_2O_3 catalysts, the MoS_2/C catalysts have a higher hydrogenating capacity, which is attainable at a lower V density. This is due to the fact that the C-supported catalysts have more mobile sulfur (surface SH groups) than the Al_2O_3-supported catalysts (apparently because the active phase in the former is more finely dispersed). Therefore, the fraction of V's per SH group in the C-supported catalysts is lower this fraction in the Al_2O_3-supported catalysts. The total number of vacancies per Mo atom in the C-supported catalysts is somewhat higher than that in the Al_2O_3-supported catalysts. These results are in good agreement with earlier data suggesting the existence of two types of the MoS_2 phase [22, 35], as in the case of the Co(Ni)-Mo-S phase. According to those data, the type I MoS_2 phase dominates in catalysts with a low Mo content and interacts strongly with the support. The type II MoS_2 phase forms in catalysts that are rich in Mo and/or are supported on an inert material.

2.2 NiMo and CoMo Promoted Catalysts Supported on Al_2O_3 and Activated Carbon

These catalysts are similar to the unpromoted catalysts in that they are sulfided to the maximum possible sulfur content corresponding to the formation of stoichiometric MoS_2 and NiS in the active phase. It follows from the data presented in

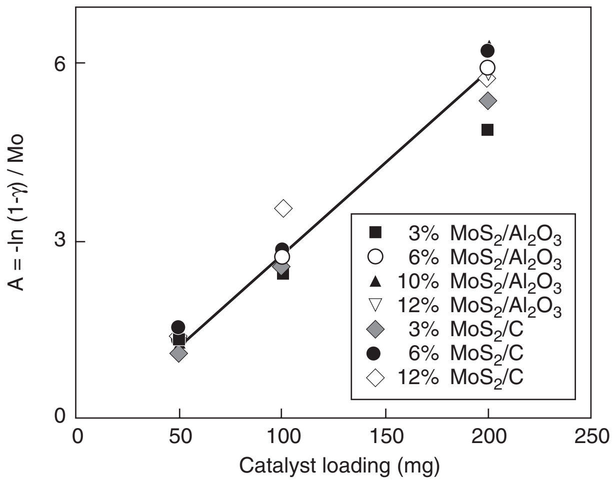

Figure 6

Specific catalytic activity $A = -\ln(1 - \gamma)/\text{Mo}$ as a function of the catalyst sample weight for the alumina- and carbon-supported molybdenum catalysts containing 3, 6, 10, and 12% Mo. γ is thiophene conversion.

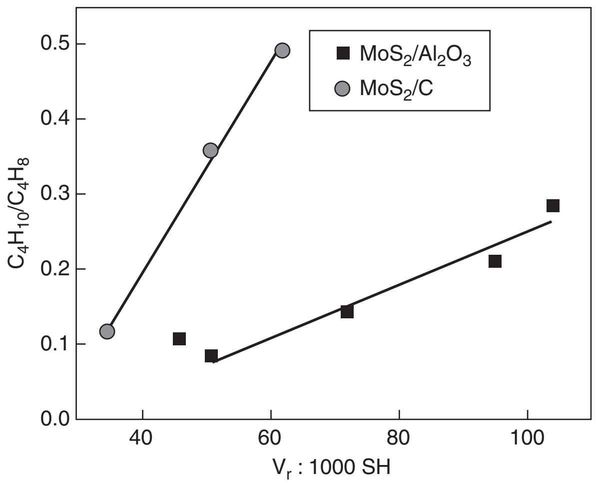

Figure 7

Hydrogenating capacity (C_4H_{10}/C_4H_8) as a function of V density (V_{rapid}/(1000 SH)) for unpromoted (■) MoS_2/Al_2O_3 and (●) MoS_2/C with different Mo contents.

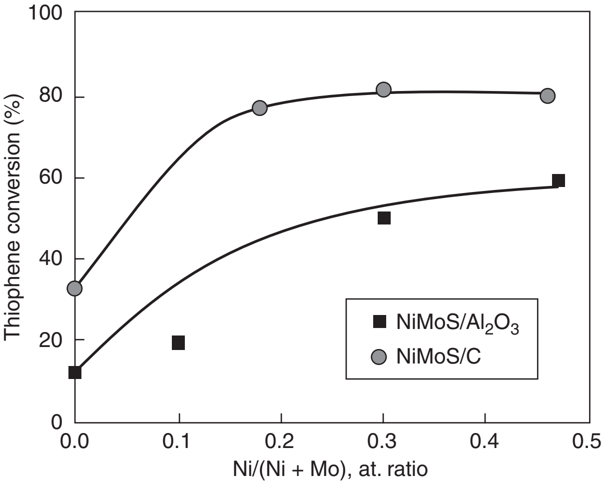

Figure 8

Thiophene conversion as a function of promoter content for the (■) Al_2O_3- and (●) C-supported NiMo sulfide catalysts.

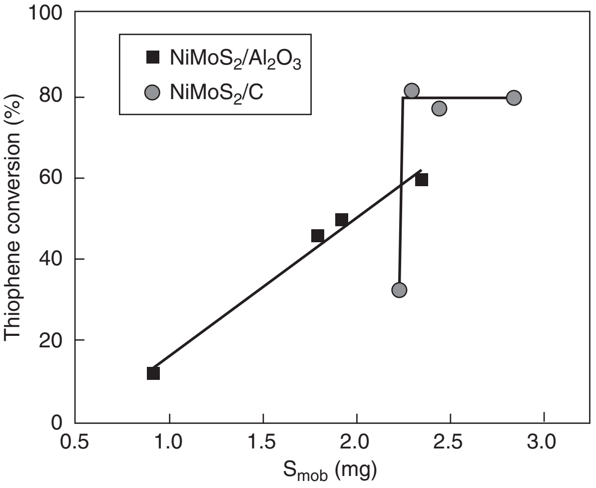

Figure 9

Thiophene conversion as a function of the amount of mobile sulfur for the (■) Al_2O_3- and (●) C-supported NiMo sulfide catalysts.

Figure 8 that the NiMoS/C catalysts are much more active in both desulfurization and hydrogenation then their Al_2O_3-supported counterparts of the same composition.

Introducing a promoter (Ni) produces different effects on catalyst activity and the ratio between conversion and the amount of mobile sulfur: for the Al_2O_3-supported catalysts, these quantities are linearly interrelated; for the C-supported catalysts, even small amounts of the promoter cause a drastic rise in catalytic activity. In the latter case, promoter concentration has only a minor effect on the mobile-sulfur content, and further raising the latter does not increase the catalytic activity *(Fig. 9)*. The unusual shape of the conversion versus mobile sulfur curve for the C-supported catalysts, particularly striking as compared with the linear dependence for the Al_2O_3-supported catalysts, apparently indicates that introduction of Ni causes qualitative changes in the active phase of the C-supported catalysts. Possible changes of this kind are alteration of the nature of active centers and redistribution of active centers caused by changes in the particle size of the active phase. It is, therefore, pertinent to make a more thorough analysis of the data relevant to the mobility and distribution of mobile sulfur in the active phase.

It was demonstrated [31] that the active phase of the $CoMo/Al_2O_3$ and $NiMo/Al_2O_3$ bimetallic catalysts has two types of surface SH group differing in capacity for forming H_2S (mobility) and, accordingly, two types of active site (AS) differing in reactivity. The more reactive sites (rapid AS's) are associated with Mo, and the less reactive sites (slow AS's) are associated with Co.

Figure 10 plots S_{mob}/Mo as a function of the promoter content r = Ni / (Ni + Mo) for the γ-Al_2O_3- and C-supported catalysts. For unpromoted Mo/Al_2O_3, $S_{mob}/Mo = 0.4$. The S_{tot}/Mo ratio in this catalyst is about 2; that is, 1/5 of the total sulfide sulfur participates in hydrogen sulfide formation. This result supports the assumption that reactive sulfur is the sulfur located on the edges of MoS_2 crystallites. The sulfide sulfur of the basal planes of alumina-supported MoS_2 crystallites is inactive. For the MoS_2/C catalyst, $S_{mob}/Mo \approx 1$, while the S/Mo ratio in molybdenum disulfide is 2. Therefore, mobile sulfur makes up only half of the total sulfide sulfur. From this, we inferred that active sulfur in MoS_2 clusters is located not only on crystallite edges but also in basal planes, probably near the crystallite edges [36]. Those regions were called rims [37] *(Fig. 11)*. It was demonstrated by EXAFS that there is weakly bonded sulfur in the basal plane of molybdenum disulfide crystallites, and it was assumed that this plane can adsorb thiophene [38].

This assumption has recently received indirect support [39]. The interaction between thiophene and flat molybdenum disulfide crystallites on a neutral (gold) support (MoS_2/Au) was studied by scanning tunneling microscopy, and it was found that thiophene is adsorbed near the edges of the basal planes of the MoS_2 crystallites. Thiophene is activated owing to the hydrogenation of the C-C bond followed by the cleavage of the C-S bond. Obviously, this pathway of the reaction is, to a considerable extent, due to the inertness of the support and the weakness of the support-active phase interaction. Similar process is possible on the basal planes of C-supported molybdenum disulfide, since the MoS_2-support interaction may be weak because of the inertness of carbon.

The fact that the number of rapid sites in the NiMo catalysts grows with increasing promoter content is in agreement with the shape of the corresponding curve for the rapid sites in the CoMo catalysts (see above). Comparing the curves for the Al_2O_3- and C-supported catalysts *(Fig. 10)* demonstrates that, as the Ni content is increased, the number of rapid AS's in the C-supported catalysts decreases markedly, while this characteristic of the Al_2O_3-supported catalysts changes little. The point is that the AS's in the basal planes of Al_2O_3-supported MoS_2 crystallites are inactive *(Fig. 11)*. Therefore, the deposition of nickel sulfide particles on the basal planes of $NiMo/Al_2O_3$ crystallites does not change the number of mobile SH groups bound to rapid AS's. For the C-supported catalysts, blocking of basal and edge sites results in a more rapid descent of the rapid-AS curve. Raising the Ni content increases the number of slow sites in the Al_2O_3- and C-supported catalysts at equal rates (the corresponding curves coincide). Therefore, catalytic activity is shown only by nickel sulfide particles situated on the edges of MoS_2 crystallites, while the particles blocking active MoS_2 sites in the basal planes do not form slow sites capable of participating in hydrogen sulfide formation.

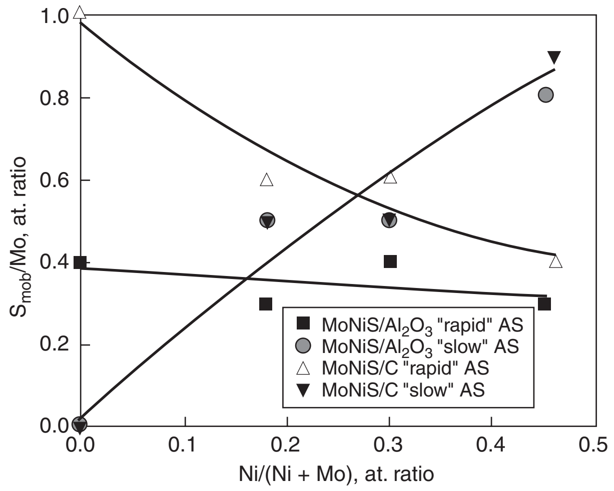

Figure 10

Mobile sulfur per gram-atom of Mo as a function of promoter content for the (■, ▲) rapid and (●, ▼) slow active sites of the (■, ●) Al_2O_3- and (▲, ▼) C-supported NiMo sulfide catalysts.

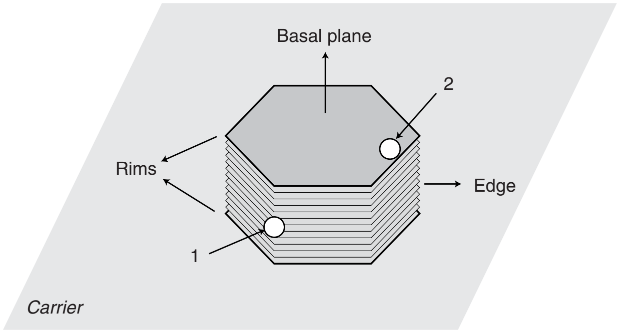

Figure 11

Schematic representation of the rim and edge model of the active phase of the MoS_2 catalyst. Adapted from [37]. The white circles are possible thiophene adsorption sites on the (1) edge and (2) basal plane.

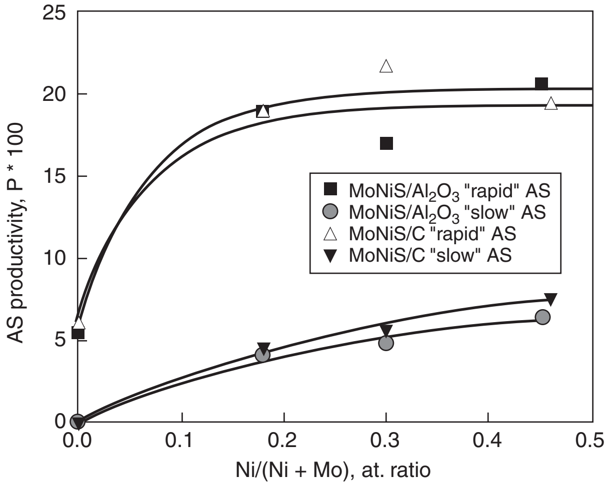

Figure 12

Productivity P of the (■, ▲) rapid and (●, ▲) slow active sites as a function of promoter content for the (■, ●) Al_2O_3- and (▲,▼) C-supported NiMo sulfide catalysts (6.87 wt% Mo).

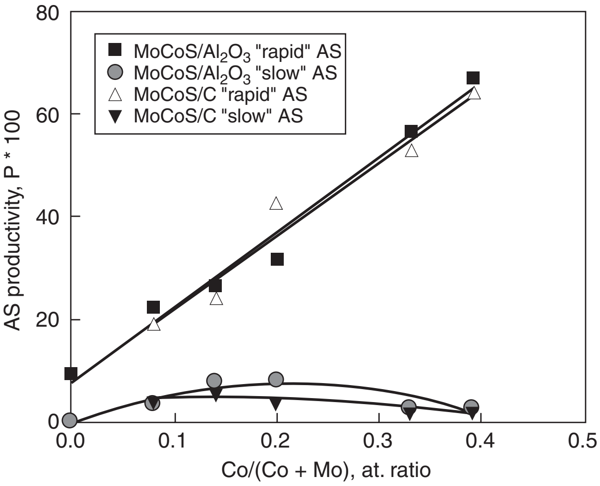

Figure 13

Productivity P of the (■, ▲) rapid and (●, ▼) slow active sites as a function of promoter content for the (■, ●) Al_2O_3- and (▲,▼) C-supported promoted CoMo sulfide catalysts (10 wt% Mo).

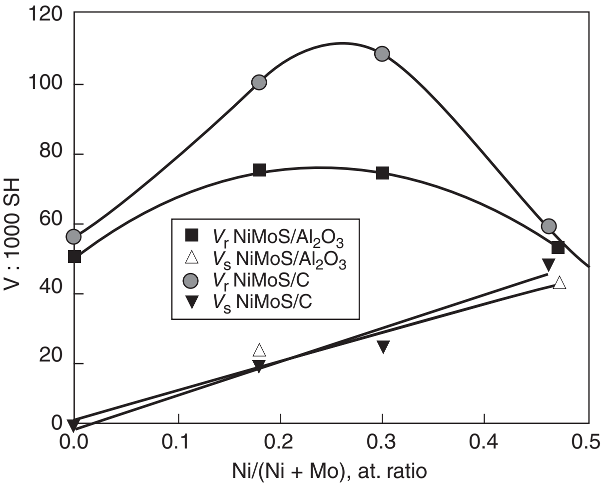

Figure 14

Density of (■, ●) rapid and (▲,▼) functioning vacancies (V) as a function of promoter content for the (■, ▲) $NiMo/Al_2O_3$ and (●, ▼) NiMo/C sulfide catalysts.

These results are consistent with productivity data as a function of promoter content *(Fig. 12)*. For the unpromoted MoS_2/Al_2O_3 and MoS_2/C catalysts, 0.05 molecules of hydrogen sulfide are formed and the same number of thiophene molecules are converted per pulse at one SH group. Therefore, every 20th (1/0.05) group takes part in hydrogen sulfide formation. These SH groups are rapid sites borne by Mo. Introducing a promoter brings about slow active sites. The productivity of both types of site increases with increasing Ni content of the active phase. At $r = 0.45$, the productivity of the rapid sites is $P_{\text{rapid}} = 0.2$: every fifth SH group belonging to the rapid sites participates in H_2S formation. For slow sites, $P_{\text{slow}} = 0.06$ at the same r, indicating that one of 16 SH groups of this type is involved in the reaction.

Coincidence of productivity versus promoter content curves for one type of AS and different supports (Al_2O_3 and carbon) is also observed for the CoMo catalysts *(Fig. 13)*. Therefore, only the number of AS's, not their nature and properties, depend on the support. Indeed, the NiMo/C catalysts have a larger number of rapid AS's than the Al_2O_3-supported catalysts of the same composition. The number of slow sites is support-independent and is determined by the amount of promoter introduced. This is particularly clear from the promoter-content dependence of the ratio of the number of V's to the number of SH groups for rapid and slow AS's in the Al_2O_3- and C-supported catalysts *(Fig. 14)*.

Since in promoted catalysts surface SH groups are not uniform and are differentiated into “rapid” and “slow” according to their mobility, anion vacancies should also be divided into those linked to “rapid” and “slow” SH groups (V_r and V_s respectively). The reasons for that are the following. According to the “forcing out” mechanism described in Introduction, one place of thiophene adsorption corresponds to one SH group that participates in H_2S formation. Participation either of a “rapid” or a “slow” SH group in H_2S formation is not a random process but is determined by the place of thiophene adsorption. That is, when thiophene is adsorbed on V_r, H_2S is formed with the participation of a “rapid” SH group; when on V_s – with the participation of a “slow” SH group. After H_2S is formed, the vacancy of the same type is formed and the balance between “rapid” and “slow” active sites is not broken. The total of vacancies is the sum of “rapid” and “slow” vacancies: $\Sigma V = \Sigma V_r + \Sigma V_s$.

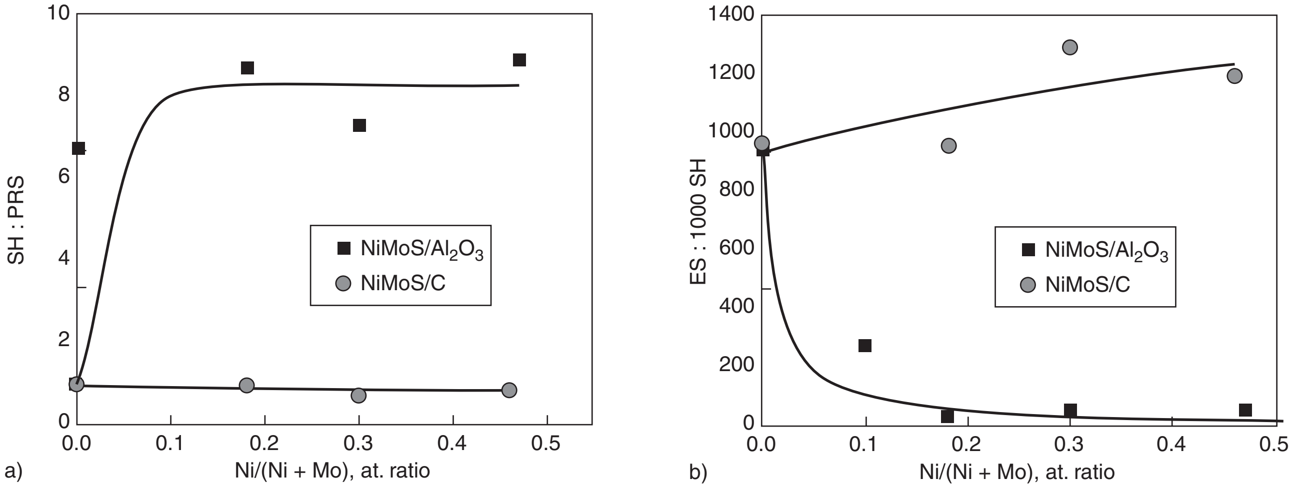

Figure15

(a) SH/PRS and (b) ES/(1000 SH) as a function of promoter content for the (■) NiMo/Al_2O_3 and (●) NiMo/C sulfide catalysts.

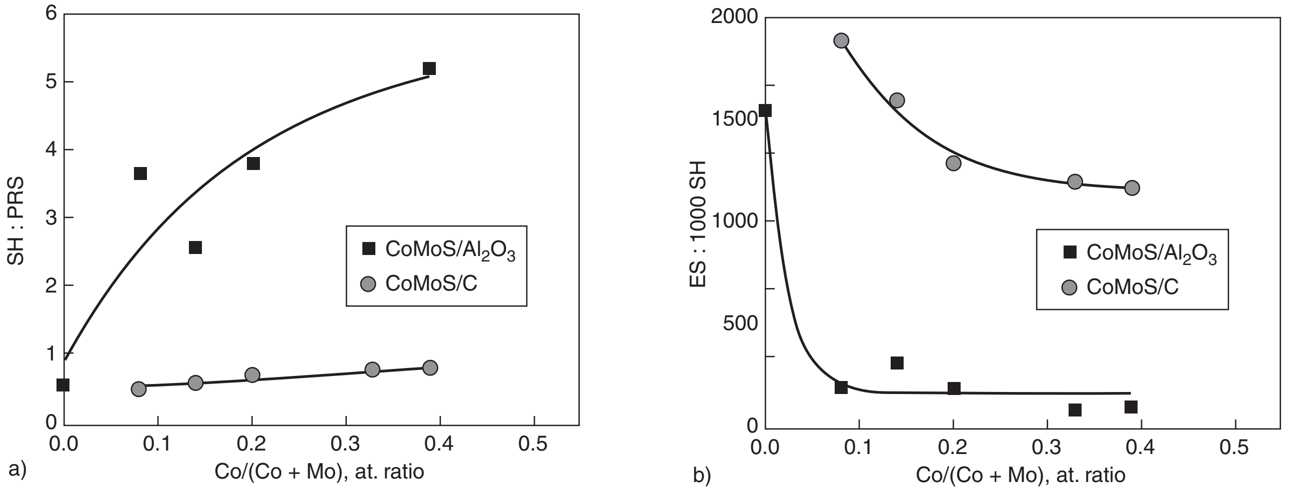

Figure 16

(a) SH/PRS and (b) ES/(1000 SH) as a function of promoter content for the (■) CoMo/Al_2O_3 and (●) CoMo/C sulfide catalysts.

The C-supported catalysts far exceed their Al_2O_3-supported counterparts in the relative number of vacancies. Both of the rapid-vacancy density (V_{rapid}) curves have a maximum near $r = 0.3$; that is, V_{rapid} peaks near the region of the NiMoS phase. The slow-vacancy density (V_{slow}) curves for the Al_2O_3- and C-supported catalysts almost coincide and ascend slowly with increasing r. Analysis of data presented in Figures 12-14, and 15a demonstrates that, in the promoted MoS_2 catalysts, the ratio between the number of surface SH groups and the number of PRS's, as well as the ratios between the number of V's, the number of ES's, and the number of SH groups, are almost independent of support nature. Introducing a small amount of Ni into the MoS_2/Al_2O_3 catalyst causes a dramatic increase in the SH coverage of surface of the active phase *(Fig. 15a)* owing to the decreasing number of ES's *(Fig. 15b)*.

This trend is shown by both Ni- and Co-promoted catalysts supported on Al_2O_3 *(Figs. 15a, 16a)*. In the C-supported catalysts, the proportion of PRS's varies little with promoter content because of the gradual variation of the fraction of empty sites *(Figs. 15b, 16b)*. This insignificant effect of the promoters on the number of PRS's is apparently

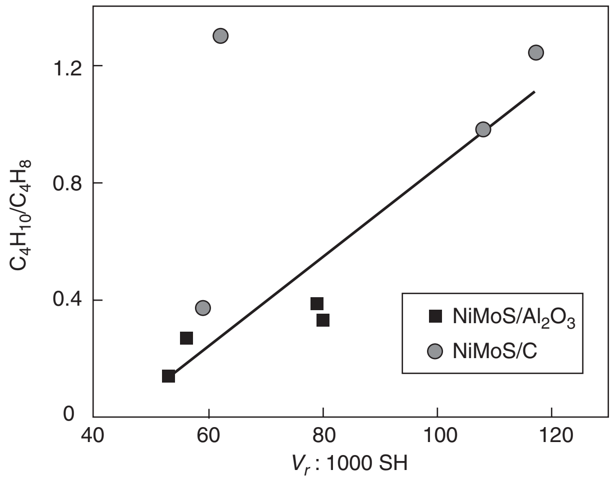

Figure 17

Hydrogenating capacity (C_4H_{10}/C_4H_8 ratio in the thiophene hydrogenolysis product) as a function of V_r density (V_{rapid}/(1000 SH)) for the (■) NiMo/Al_2O_3 and (●) NiMo/C sulfide catalysts.

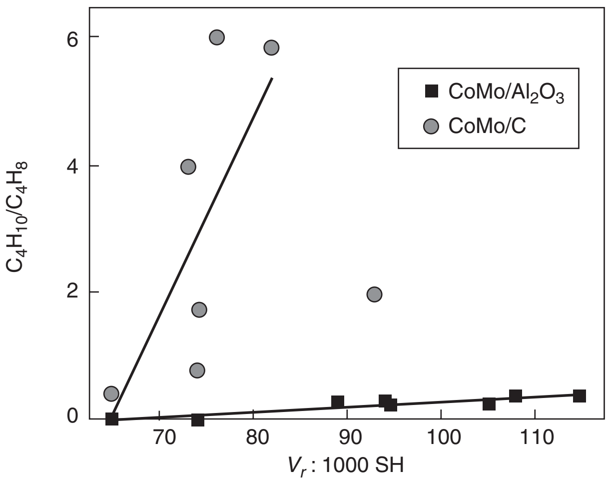

Figure 18

Hydrogenating capacity (C_4H_{10}/C_4H_8 ratio in the thiophene hydrogenolysis product) as a function of V_r density (V_{rapid}/(1000 SH)) for the (■) CoMo/Al_2O_3 and (●) CoMo/C sulfide catalysts.

due to the fact that the support and the active phase in the C-supported catalysts interact weakly, irrespective of whether a promoter is present. As a consequence, the C-supported catalysts have a lower SH coverage of the active-phase surface and a larger fraction of ES's than the Al_2O_3-supported catalysts.

The hydrogenation activity of the C-supported Mo and NiMo catalysts is higher than that of their Al_2O_3-supported counterparts. The linear dependence of the hydrogenation activity of the catalyst (C_4H_{10}/C_4H_8) on the density of rapid V's (V_{rapid}/(1000 SH)) *(Fig. 17)* suggests that both the hydrogenating and desulfurizing properties of the active sites are determined only by the number of these sites and are support-independent.

The hydrogenation activity the CoMoS phase, unlike that of the NiMo catalysts, is support-dependent, as in the case of the unpromoted $MoS_2/Al_2O_3$and MoS_2/C catalysts *(Fig. 7)*. As is clear from Figures 17 and 18, the C-supported CoMoS catalysts exceed the Al_2O_3- supported ones in the amount of mobile sulfur (number of surface SH groups). Therefore, the number of rapid V's (V_{rapid}) per SH group is smaller in the C-supported catalysts than in the Al_2O_3-supported catalysts. However, the total number of V's in the C-supported catalysts is 3-5 times higher than that in their Al_2O_3-supported counterparts with the same composition of the active phase.

In other terms, the NiMoS phase forms on both carbon and alumina and is apparently a type II phase. The CoMoS phase on carbon is always type II. The CoMoS phase on alumina can be either type I or type II, depending on the catalyst composition, preparation conditions, and the properties of the support.

CONCLUSIONS

The main results of the comparative study of the alumina and carbon- supported Mo and Ni(Co)Mo sulfide catalysts are the following:

- The C-supported catalysts contain more mobile sulfur than the Al_2O_3-supported catalysts because of the smaller particle size of the active phase.
- The SH/PRS ratio in the C-supported catalysts is much smaller than that in the Al_2O_3-supported catalysts, suggesting that the active phase in the former is reduced to a greater extent. Raising the Mo content reduces SH/PRS in both the Al_2O_3- and C-supported catalysts.
- The Al_2O_3- and C-supported catalysts are similar in the productivity of the active sites. Therefore, these sites are of the same nature. The productivity of the active sites depends on the promoter content of the active phase and is support-independent.
- The dynamic properties of the active sites in the NiMo and CoMo catalyst are similar.
- The hydrogenation of butenes that have resulted from thiophene hydrogenolysis takes place on sites that are associated with Mo and responsible for desulfurization.

ACKNOWLEDGEMENTS

This work has been supported by the Russian Federation for Basic Research – RFBR grant 05-03-3906-a.

REFERENCES

1 de Beer, V.H.J., Duchet, J.C. and Prins, R. (1981) The role of cobalt and nickel in hydrodesulfurization: promoters or catalysts? *J. Catal.*, **72**, 2, 369–372.

2 Duchet, J.C., van Oers, E.M., de Beer, V.H.J. and Prins, R. (1983) Carbon-supported sulfide catalysts. *J. Catal.*, **80**, 2, 386–402.

3 Scheffer, B., Arnoldy, P. and Moulijn, J.A. (1988) Sulfidability and hydrodesulfurization activity of Mo catalysts supported on alumina, silica, and carbon. *J. Catal.*, **112**, 516–527.

4 Farag, H., Mochida, I. and Sakanishi, K. (2000) Fundamental comparison studies on hydrodesulfurization of dibenzothiophenes over CoMo-based carbon and alumina catalysts. *Appl. Catal. A–Gen.*, **194**, 147–157.

5 Hillerová, E., Vít, Z., Zdražil, M., Shkuropat, S.A., Bogdanets, E.N. and Startsev, A.N. (1991) Comparison of carbon and alumina supported nickel-molybdenum sulfide catalysts in parallel hydrodenitrogenation and hydrodesulphurization. *Appl. Catal.*, **67**, 231–236.

6 Farag, H., Whitehurst, D.D., Sakanishi, K. and Mochida, I. (1999) Carbon versus alumina as a support for Co-Mo catalysts reactivity towards HDS of dibenzothiophenes and diesel fuel. *Catal. Today*, **50**, 9–17.

7 Bouwens, S.M.A.M., van Zon, F.B.M., van Dijk, M.P., van der Kraan, A.M., de Beer, V.H.J., van Veen, J.A.R. and Koningsberger, D.C. (1994) On the structural differences between alumina-supported CoMoS Type-I and alumina-supported, silica-supported, and carbon-supported CoMoS Type-II phases studied by XAFS, MES, and XPS. *J. Catal.*, **146**, 375–393.

8 Laine, J., Labady, M., Severino, F. and Yunes, S. (1997) Sink effect in activated carbon-supported hydrodesulfurization catalysts, *J. Catal.*, **166**, 384–387.

9 Severino, F., Laine, J. and Lopez-Agudo, A. (2000) Compensation effect and dual promotion effect in activated carbon-supported CoNiMo hydrodesulfurization catalysts. *J. Catal.*, **189**, 244–246.

10 Visser, J.P.R., de Beer, V.H.J. and Prins, R. (1987) The role of cobalt in sulfidized cobalt-molybdenum hydrodesulfurization catalysts supported on carbon and alumina. *J. Chem. Soc. Faraday T.*, **1**, 83, 2145–2155.

11 Visser, J.P.R., Scheffer, B., de Beer, V.H.J., Moulijn, J.A. and Prins, R. (1987) Effect of the support on the structure of Mo-based hydrodesulfurization catalysts-activated carbon versus alumina. *J. Catal.,* **105**, 2, 277–284.

12 Bouwens, S.M.A.M., Koningsberger, D.C., de Beer, V.H.J. and Prins, R. (1987) An EXAFS study on carbon-supported Mo and Co-Mo sulfide by hydrodesulphurization catalysts. *B. Soc. Chim. Belg.*, **96**, 951–959.

13 Crajé, M.W.J. (1992) *On the identification of "Co-sulfide" species in sulfided Co and CoMo catalysts.* PhD Thesis, TU Delft.

14 Muralidhar, G., Concha, B.E., Bartholomew, G.L. and Bartholomew, C.H. (1984) Characterization of reduced and sulfided, supported molybdenum catalysts by oxygen chemisorption, X-ray diffraction, and ESCA. *J. Catal.*, **89**, 274–284.

15 Alstrup, I., Chorkendorff, I., Candia, R., Clausen, B.S. and Topsøe, H. (1982) A combined X-ray photoelectron and Mössbauer emission spectroscopy study of the state of cobalt in sulfided, supported, and unsupported cobalt-molybdenum catalysts. *J. Catal.*, **77**, 397–409.

16 Bouwens, S.M.A.M., Koningsberger, D.C., de Beer, V.H.J. and Prins, R. (1991) Extended X-Ray absorption fine structure determination of the structure of cobalt in carbon-supported CO and CO-Mo Sulfide Hydrodesulfurization Catalysts. *J. Phys. Chem.*, **95**, 123–134.

17 van der Kraan, A.M., Crajé, M.W.J., Gerkema, E., Ramselaar, W.L.T.M. and de Beer, V.H.J. (1988) So-called Co-Mo-S phase observed in carbon-supported cobalt sulfide catalyst by Mössbauer emission-spectroscopy. *Appl. Catal.*, **39**, 1-2, L7–L10.

18 Crajé, M.W.J., Louwers, S.P.A., de Beer, V.H.J., Prins, R. and van der Kraan, A.M. (1992) An EXAFS study on the so-called Co-Mo-S phase in Co/C and CoMo/C, compared with a Mössbauer emission spectroscopy study. *J. Phys. Chem.*, **95**, 5445–5452.

19 Breysse, M., Bennett, B.A., Chadwick, D. and Vrinat, M. (1981) Structure and HDS activity of Co-Mo catalysts: A comparison of alumina and carbon supports. *B. Soc. Chim. Belg.* **90**, 1271–1277.

20 Topsøe, H. and Clausen, B.S. (1984) Importance of Co-Mo-S type structures in hydrodesulphurization. *Catal. Rev.*, **26**, 395–420.

21 Topsøe, H. and Clausen, B.S. (1986) Active-sites and support effects in hydrodesulfurization catalysts. *Appl. Catal.*, **25**, 273–293.

22 Candia, R., Villadsen, J., Topsøe, N.-Y., Clausen, B.S. and Topsøe, H. (1984) Effect of sulfiding temperature on activity and structures of Co-Mo/Al_2O_3 catalysts. *B. Soc. Chim. Belg.*, **93**, 763–773.

23 Pawelec, B., Mariscal, R., Fierro, J.L.G., Greenwood, A. and Vasudevan, P.T. (2001) Carbon-supported tungsten and nickel catalysts for hydrodesulfurization and hydrogenation reactions. *Appl. Catal.,* **206**, 295–307.

24 Hensen, E.J.M., Brans, H.J.A., Lardinois, G.M.H.J., de Beer, V.H.J., van Veen, J.A.R. and van Santen, R.A. (2000) Periodic trends in hydrotreating catalysis: thiophene hydrodesulfurization over carbon-supported 4d transition metal sulfides. *J. Catal.*, **192**, 98–107.

25 Sakanishi, K., Nagamatsu, T., Mochida, I. and Duayne Whitehurst, D. (2000) Hydrodesulfurization kinetics and mechanism of 4,6-dimethyldibenzothiophene over NiMo catalyst supported on carbon. *J. Mol. Catal. A–Chem.*, **155**, 101–109.

26 Ferrari, M., Maggi, R., Delmon, B. and Grange, P. (2001) Influences of the hydrogen sulfide partial pressure and of a nitrogen compound on the hydrodeoxygenation activity of a CoMo/carbon catalyst. *J. Catal.*, **198**, 47–55.

27 Farag, H., Mochida, I. and Sakanishi, K. (2000) Fundamental comparison studies on hydrodesulfurization of dibenzothiophenes over CoMo-based carbon and alumina catalysts. *Appl. Catal. A–Gen.*, **194-195**, 147–157.

28 Lee, J.J., Han, S., Kim, H., Koh, J.H., Hyeon, T. and Moon, S.H. (2003) Performance of CoMoS catalysts supported on nano-porous carbon in the hydrodesulfurization of dibenzothiophene and 4,6-dimethyldibenzothiophene. *Catal. Today,* **86**, 141–149.

29 Kogan, V.M., Rozhdestvenskaya, N.N. and Korshevets, I.K. (2002) Radioisotopic study of CoMo/Al_2O_3 sulfide catalysts for HDS. Part I. Active site monitoring. *Appl. Catal. A–Gen.,* **234**, 207–219.

30 Kogan, V.M., Parfenova, N.M., Gaziev, R.G., Rozhdestvenskaya, N.N. and Korshevets, I.K. (2003) *In situ* radioisotopic study of the active sites of sulfide CoMo catalysts and the mechanism of thiophene hydrodesulphurization. *Kinet. Catal.*, **44** (4) 583–599.

31 Kogan, V.M., Gaziev, R.G., Lee, S.W. and Rozhdestvenskaya, N.N. (2003) Radioisotopic study of CoMo/Al_2O_3 Sulfide Catalysts for HDS: Part III. Poisoning by N-containing compounds. *Appl. Catal. A–Gen.*, **251**, 187–198.

32 Cristol, S., Paul, J.F., Payen, E., Bougeard, D., Hafner, J. and Hutschka, F. (1999) Theoretical study of benzothiophene hydrodesulfurization on MoS_2. *Stud. Surf. Sci. Catal.*, **127**, 327–334.

33 Schweiger, H., Raybaud, P., Kresse, G. and Toulhoat, H. (2002) Shape and edge sites modifications of MoS_2 catalytic nanoparticles induced by working conditions: A theoretical study. *J. Catal.*, **207**, 76–87.

34 Schweiger, H., Raybaud, P. and Toulhoat, H. (2002) Promoter sensitive shapes of Co(Ni)MoS nanocatalysts in sulfo- reductive conditions. *J. Catal.*, **212**, 33–38.

35 Miciukiewicz, J. and Massoth, F.E. (1989) Studies of molybdena alumina catalysts .16. Effect of high temperature sulfiding. *J. Catal.*, **119**, 531–533.

36 Kogan, V.M., Thi Dung Nguen and Yakerson, V.I. (1995) Comparative study of sulfide Ni-Mo catalysts, supported on γ-Al_2O_3 and activated carbon by using ^{35}S. *B. Soc. Chim. Belg.*, **104**, 303–309.

37 Daage, M. and Chianelli, R.R. (1994) Structure-function relations in molybdenum sulfide catalysts – the rim-edge model. *J. Catal.*, **149**, 414–427.

38 Kochubey, D.I. and Babenko, V.P. (2002) Structure of MoS_2-based catalysts for hydrodesulfurization prepared via exfoliation. *React. Kinet. Catal. L.*, **77** (2), 237–243.

39 Lauritsen, J.V., Nyberg, M., Vang, R.T., Bollinger, M.V., Clausen, B.S., Topsøe, H., Jacobsen, K.W., Lgsgaard, E., Norskov, J.K. and Besenbacher, F. (2003) Chemistry of one-dimensional metallic edge states in MoS_2 nanoclusters. *Nanotechnology*, **14**, 385–389.

Final manuscript received in June 2006